Directional PCA for Fast Detection and Accurate Diagnosis: A Unified Framework

Jian Li, *Member, IEEE*, Dong Ding, and Fugee Tsung

***Abstract*—Many methods for monitoring multivariate processes are built on principal component analysis (PCA), which, however, simply tells whether the process is faulty or not. In fact, there is still room for the improvement of the early detection performance by exploiting fully the information given by fault directions. To this end, this article proposes a novel directional PCA (diPCA) approach. First, by narrowing down faults to a specified direction or composite mutually orthogonal directions, diPCA can speed fault detection and facilitate accurate fault diagnosis. It also has good theoretical properties that guarantee concise control limits. Second, with appropriate fault directions, diPCA provides a unified framework for process monitoring and includes existing monitoring indices, such as Hotelling's T^2 and the squared prediction error (SPE), as special cases. Third, diPCA also naturally results in a new combined monitoring statistic, which is composed of both T^2 and SPE, and provides an optimal ratio of their combination. The Monte Carlo simulation results have demonstrated the power of the proposed monitoring and diagnostic methods stemming from diPCA. The proposed methods have also been implemented into the Tennessee Eastman process.**

***Index Terms*—Composite hypothesis, fault direction, likelihood ratio test (LRT), normalization, probabilistic principal component analysis (PCA) model.**

I. Introduction

WITH THE explosion in the use of sensors, data-driven process monitoring and diagnostic approaches are prevailing in complex industrial processes because they are easy to implement and highly efficient. By exploiting information in the collected data effectively, they can detect and identify process faults and are, therefore, critical to process stability. Among various techniques, many principal component analysis (PCA)-based methods have been developed for fault detection and diagnosis [1]–[3], as well as for condition monitoring [4]–[6]. PCA preserves the most information about variability in the original high-dimensional data in the principal component subspace, and the residual subspace mainly comprises noise [7], [8]. In the two orthogonal subspaces, Hotelling's T^2 statistic and the squared prediction error (also known as Q) are established. There are also indices that combine T^2 and Q in some manner, which are preferable to using T^2 or Q separately. See [9]–[13] for detailed overviews.

Many PCA-based detection approaches simply indicate whether the process is faulty or not, but there is still room to improve the performance for early detection. The performance is measured by the average run length (ARL), which is the average number of samples before an alarm is triggered online. Given the Type I error probability α, a smaller ARL indicates better performance by a method, that is, it detects a fault earlier or faster than other approaches. The motivation of this article is to improve the detection performance of PCA-based approaches by exploiting the information in fault directions fully, leading to directional PCA (diPCA). Conventional PCA fails to consider such directional information, whereas diPCA assumes the fault lies in one of the mutually orthogonal directions, which is common in practice. Therefore, diPCA focuses on faults in these directions, thereby enabling greater detection power.

Directional information has been considered previously in fault diagnosis. Alcala and Qin [14] proposed a reconstruction-based contribution (RBC) approach for fault diagnosis. The RBC method calculates an RBC index for single-sensor faults in each possible direction, and the direction with the largest index is considered to be faulty. In [14], the Monte Carlo simulations and rigorous diagnosability analysis were performed to demonstrate that this RBC approach has much better diagnostic performance than conventional contribution plots [15] that have a smearing effect leading to misdiagnosis [9]. In addition to the linear models considered, in [16], the RBC method was also extended to nonlinear principal component models by incorporating kernel PCA.

However, incorporating fault directions into PCA-based monitoring statistics poses a challenge, which is challenging compared to the RBC method for diagnosis. Furthermore, there are drawbacks to conventional PCA-based monitoring indices. For instance, some combined monitoring indices of T^2 and Q contain extra parameters that are yet to be

Manuscript received July 8, 2020; revised December 7, 2020 and March 8, 2021; accepted March 26, 2021. This work was supported in part by the National Key R&D Program of China under Grant 2019YFB1704100; in part by the National Natural Science Foundation of China under Grant 71772147, Grant 71602155, and Grant 71931006; in part by the Hong Kong RGC General Research Funds under Grant 16216119 and Grant 16201718; in part by the Science and Technology Innovation Team Plan of Shaanxi Provience under Grant S2020-ZC-TD-0083; and in part by the Youth Innovation Team of Shaanxi Universities "Big Data and Business Intelligent Innovation Team." This article was recommended by Associate Editor S. Cruces. *(Corresponding author: Jian Li.)*

Jian Li is with the School of Management and State Key Laboratory for Manufacturing Systems Engineering, Xi'an Jiaotong University, Xi'an 710049, China (e-mail: jianli@xjtu.edu.cn).

Dong Ding is with the School of Management, Xi'an Polytechnic University, Xi'an 710048, China (e-mail: laceyding@foxmail.com).

Fugee Tsung is with the Department of Industrial Engineering and Decision Analytics, Hong Kong University of Science and Technology, Hong Kong (e-mail: season@ust.hk).

Digital Object Identifier 10.1109/TCYB.2021.3070590

determined, such as the significance level α in the combined index proposed by Yue and Qin [17] and α and c in the combined statistic in [18]. Different values of α and c lead to different detection performances. Another example is the control limit of the Q statistic proposed by Jackson and Mudholkar [19], which is widely used but difficult to calculate. The same can also be said for that of the combined statistic in [17].

In order to exploit directional information about faults sufficiently, here process monitoring is formulated as a hypothesis testing problem. Some works have also combined PCA with hypothesis testing [20], [21], but fault directions were not considered. In fact, various patterns of fault directions can be incorporated in the alternative hypotheses, which have sufficient flexibility, and a statistic for detecting faults with such directions can be further derived.

Based on hypothesis testing, the next step is to find a probability model that is related to PCA and allows the testing of such hypotheses. Fortunately, probabilistic PCA (PPCA) provides such a probability model. PPCA was proposed by Tipping and Bishop [22], which focused on the maximum-likelihood estimation and statistical properties of PPCA. This work is the basis of other papers that utilize PPCA for fault detection and diagnosis, including [23]–[25]. Please be reminded that there is a lack of an associate probabilistic model for the observed data in conventional PCA. Instead, PPCA relates the observed data to a Gaussian latent variable model, and the principal subspace can be determined by maximum-likelihood estimation of parameters in the PPCA model. Furthermore, the likelihood ratio test (LRT) statistic can be derived to test whether the process is faulty, where the hypothesis involves a specified fault direction or composite mutually orthogonal fault directions.

This article does not follow [23]–[25], which first estimates the posterior mean and covariance matrix of the latent vector based on the observed data in a Bayesian manner, and then constructs corresponding T^2-type and Q-type statistics separately using these posterior estimates. Instead, like [26], this article operates in a frequentist way and integrates the latent vector out. By including fault directions in the hypothesis, the LRT for the PPCA model leads to diPCA for process monitoring.

This article will make the following three specific contributions. First, by narrowing down faults to a specified direction or composite mutually orthogonal directions, diPCA can speed fault detection and facilitate accurate fault diagnosis. Second, with appropriate fault directions, diPCA provides a unified framework for process monitoring and includes existing monitoring indices, such as T^2 and Q, as special cases. Third, diPCA also naturally results in a new combined monitoring statistic W composed of both T^2 and Q simultaneously, free from extra parameters. This W also provides an optimal ratio of T^2 and Q of their combination. In addition, diPCA has nice theoretical properties, which guarantee concise control limits of both Q and W.

The remaining sections are organized as follows. Section II briefly summarizes conventional PCA-based methods and introduces the PPCA model. Section III elaborates on diPCA and composite diPCA (cdiPCA) for process monitoring, as well as the resulting accurate diagnostic scheme. Section IV investigates the performance of the proposed approaches for process monitoring and diagnosis, which is measured by ARLs and matching rates, respectively. Section V illustrates the implementation of the proposed schemes into the well-known Tennessee Eastman (TE) process, and Section VI concludes this article.

II. Probabilistic PCA

A. Conventional Process Monitoring via PCA

PCA is a powerful dimension reduction technique that preserves the most variability information in original high-dimensional data. Given the off-line dataset collected in the normal operating condition, the observation vectors, each of dimension p, are scaled to zero mean and unit variance. Denote the covariance matrix of the dataset by $\mathbf{\Omega}$. The PCA-based process monitoring methods require the eigenvalue decomposition of $\mathbf{\Omega}$, which is

$$\mathbf{\Omega} = \left[\boldsymbol{U}, \widetilde{\boldsymbol{U}}\right] \mathbf{\Lambda} \left[\boldsymbol{U}, \widetilde{\boldsymbol{U}}\right]^T. \tag{1}$$

Here, the $p \times p$ matrix $[\boldsymbol{U}, \widetilde{\boldsymbol{U}}]$ is the loading matrix, containing the columnwise eigenvectors of $\mathbf{\Omega}$, and

$$\mathbf{\Lambda} = \operatorname{diag}\left\{\lambda_1, \ldots, \lambda_q, \lambda_{q+1}, \ldots, \lambda_p\right\} \tag{2}$$

is a diagonal matrix with the eigenvalues of $\mathbf{\Omega}$ as its diagonal elements in descending order, that is, $\lambda_1 \geq \cdots \geq \lambda_p > 0$. Moreover

$$\boldsymbol{U} = \left[\mathbf{u}_1, \ldots, \mathbf{u}_q\right] \quad \text{and} \quad \widetilde{\boldsymbol{U}} = \left[\mathbf{u}_{q+1}, \ldots, \mathbf{u}_p\right] \tag{3}$$

consist of the eigenvectors, with the eigenvector $\mathbf{u}_j$ corresponding to λ_j. Here, q is the number of principal components determined by some criteria in [13], such as the cumulative percentage of variance (CPV).

For a new observation vector $\mathbf{x}$ of dimension p, let

$$\mathbf{\Lambda}_q = \operatorname{diag}\left\{\lambda_1, \ldots, \lambda_q\right\} \tag{4}$$

and the Hotelling's T^2 statistic and Q statistic are

$$T^2 = \mathbf{x}^T \boldsymbol{U} \mathbf{\Lambda}_q^{-1} \boldsymbol{U}^T \mathbf{x} \tag{5}$$

$$Q = \mathbf{x}^T \widetilde{\boldsymbol{U}} \widetilde{\boldsymbol{U}}^T \mathbf{x}. \tag{6}$$

Unlike T^2, the Q statistic does not involve the eigenvalues $\lambda_{q+1}, \ldots, \lambda_p$ corresponding to $\widetilde{\boldsymbol{U}}$. In fact, $\widetilde{\boldsymbol{U}}$ determines the residual subspace, which usually has little variability information and mainly contains noise. Therefore, the last $p-q$ eigenvalues are usually very small or near zero compared to the leading q eigenvalues, and their inverses often lead to large biases due to the estimation inaccuracy of matrix $\mathbf{\Omega}$ [9].

In process monitoring, one usual detection scheme is to see whether at least one of T^2 and Q exceeds their corresponding control limits J_{α,T^2} and $J_{\alpha,Q}$, respectively, where α is the significance level. Since in the normal case, T^2 follows asymptotically the chi-square distribution with q degrees of freedom (d.f.), χ_q^2, J_{α,T^2} is the $(1-\alpha)$-quantile of χ_q^2. In addition, Jackson and Mudholkar [19] provided an expression of $J_{\alpha,Q}$.

If both T^2 and Q are within their control limits, it is fault-free. Otherwise, it is faulty. This joint monitoring approach is hereafter referred to as T^2-Q.

One can also employ a combined index [17]

$$\frac{T^2}{J_{\alpha,T^2}} + \frac{Q}{J_{\alpha,Q}} \tag{7}$$

for process monitoring, which is the sum of T^2 and Q divided by their α-level thresholds, respectively. This method is referred to as "combined."

B. Probabilistic PCA Model

To improve the detection power of PCA-based process monitoring methods, as suggested in the introduction, here, the PPCA model proposed by Tipping and Bishop [22] is introduced to incorporate various fault directions into hypothesis testing. The PPCA model assumes a group of latent variables of the observed high-dimensional variables. To be specific, in the normal case, the observed vector $\mathbf{x}$ is determined by

$$\mathbf{x} = \boldsymbol{A}\mathbf{z} + \boldsymbol{\epsilon} \text{ with } \mathbf{z} \sim \mathrm{N}\big(\mathbf{0}; \mathbf{I}_q\big) \text{ and } \boldsymbol{\epsilon} \sim \mathrm{N}\big(\mathbf{0}; \sigma\mathbf{I}_p\big) \tag{8}$$

where $\mathbf{z}$ is the latent factor vector of dimension $q < p$, independently subject to a multivariate normal distribution with zero mean and unit variance, and the $p \times q$ link matrix $\boldsymbol{A}$ relates $\mathbf{x}$ to $\mathbf{z}$. In addition, $\boldsymbol{\epsilon}$ is the $p \times 1$ measurement or sensor error vector subject to a multivariate normal distribution, independently with zero mean and identical variance $\sigma > 0$. With $q < p$, the latent vector $\mathbf{z}$ provides a parsimonious explanation of the dependence between the high-dimensional vector $\mathbf{x}$. By integrating $\mathbf{z}$ out, the distribution of $\mathbf{x}$ can be finally derived as

$$\mathrm{N}\big(\mathbf{0}; \boldsymbol{A}\boldsymbol{A}^T + \sigma\mathbf{I}_p\big) \tag{9}$$

that is, the multivariate normal distribution with zero mean and covariance matrix $\boldsymbol{A}\boldsymbol{A}^T + \sigma\mathbf{I}_p$.

The parameters of the PPCA model can be estimated using maximum-likelihood estimation. According to [22], $\boldsymbol{A}$ and σ are estimated as

$$\boldsymbol{A} = \boldsymbol{U}\big(\boldsymbol{\Lambda}_q - \sigma\mathbf{I}_q\big)^{1/2}\boldsymbol{R} \tag{10}$$

$$\sigma = \frac{1}{p-q}\sum_{j=q+1}^{p}\lambda_j = \frac{\mathrm{tr}(\boldsymbol{\Omega}) - \sum_{j=1}^{q}\lambda_j}{p-q} \tag{11}$$

where q, $\boldsymbol{U}$, $\boldsymbol{\Lambda}_q$, and λ_i $(i = 1, \ldots, p)$ are all associated with the eigenvalue decomposition of $\boldsymbol{\Omega}$ expressed in (1), and $\boldsymbol{R}$ of dimension $q \times q$ is an arbitrary orthogonal rotation matrix.

III. Directional PCA for Processing Monitoring and Diagnosis

A. Directional PCA

The PPCA model is based on a probability distribution, which allows the use of some statistical tests for process monitoring. The likelihood ratio test is flexible and powerful when comparing the goodness-of-fit of two statistical models: 1) a null model and 2) an alternative one. Therefore, it can be employed to detect whether the process is normal or faulty.

When a fault occurs, say fault i, the faulty observation vector can be expressed as

$$\mathbf{x} = \mathbf{x}^* + \boldsymbol{\Xi}_i\mathbf{f}_i. \tag{12}$$

Here, $\mathbf{x}^*$ is an observation vector in the normal case, $\boldsymbol{\Xi}_i$ of dimension $p \times r_i$ $(r_i \le p)$ is the fault direction matrix with orthogonal columns satisfying $\boldsymbol{\Xi}_i^T\boldsymbol{\Xi}_i = \mathbf{I}_{r_i}$ and spanning the fault subspace, and vector $\mathbf{f}_i$ represents the fault magnitude. In the context of LRT, let $\boldsymbol{\mu}$ be the mean vector of observation vectors, the fault detection problem can be formulated by testing the following hypothesis:

$$H_0 : \boldsymbol{\mu} = \mathbf{0} \quad \text{versus} \quad H_1 : \boldsymbol{\mu} = \boldsymbol{\Xi}_i\mathbf{f}_i. \tag{13}$$

Assume that the fault direction matrix $\boldsymbol{\Xi}_i$ is known. Given the PPCA model, the observation vector $\mathbf{x}$ is subject to the multivariate normal distribution with mean vector $\Xi_i\mathbf{f}_i$ and covariance matrix $\boldsymbol{\Sigma}$, namely, $\mathrm{N}(\Xi_i\mathbf{f}_i; \boldsymbol{\Sigma})$. Thus, the probability density function (PDF) of $\mathbf{x}$, that is, $p(\mathbf{x}|\mathbf{f}_i)$, or equivalently, the likelihood function $L(\mathbf{f}_i|\mathbf{x})$ can be written from the PDF of the multivariate normal distribution as

$$\begin{aligned} p(\mathbf{x}|\mathbf{f}_i) &= L(\mathbf{f}_i|\mathbf{x}) \\ &= \frac{1}{\sqrt{(2\pi)^p|\boldsymbol{\Sigma}|}}\exp\left(-\frac{1}{2}(\mathbf{x} - \boldsymbol{\Xi}_i\mathbf{f}_i)^T\boldsymbol{\Sigma}^{-1}(\mathbf{x} - \boldsymbol{\Xi}_i\mathbf{f}_i)\right) \end{aligned} \tag{14}$$

with

$$\boldsymbol{\Sigma} = \boldsymbol{A}\boldsymbol{A}^T + \sigma\mathbf{I}_p = \boldsymbol{U}\boldsymbol{\Lambda}_q\boldsymbol{U}^T + \sigma\big(\mathbf{I}_p - \boldsymbol{U}\boldsymbol{U}^T\big). \tag{15}$$

Note that $\boldsymbol{\Sigma}$ is not necessarily identical to $\boldsymbol{\Omega}$ in (1). In fact, $\boldsymbol{\Omega}$ is the calculated covariance matrix based on the off-line dataset, whereas $\boldsymbol{\Sigma}$ is the normal-case covariance matrix associated with the PPCA model (8).

By maximizing $\ln L(\mathbf{f}_i|\mathbf{x})$, the maximum-likelihood estimate of $\mathbf{f}_i$ is

$$\widehat{\mathbf{f}}_i = \Big(\boldsymbol{\Xi}_i{}^T\boldsymbol{\Sigma}^{-1}\boldsymbol{\Xi}_i\Big)^{-1}\boldsymbol{\Xi}_i{}^T\boldsymbol{\Sigma}^{-1}\mathbf{x}. \tag{16}$$

The LRT first computes the maximum-likelihood functions under the null and alternative hypotheses, which are $L(\mathbf{0}|\mathbf{x})$ and $L(\widehat{\mathbf{f}}_i|\mathbf{x})$, respectively. It then takes their ratio, denoted by λ, and uses $-2\ln\lambda$ as the test statistic, which is

$$\begin{aligned} R_i &= -2\ln\frac{L(\mathbf{0}|\mathbf{x})}{L\big(\widehat{\mathbf{f}}_i|\mathbf{x}\big)} \\ &= \mathbf{x}^T\boldsymbol{\Sigma}^{-1}\boldsymbol{\Xi}_i\Big(\boldsymbol{\Xi}_i{}^T\boldsymbol{\Sigma}^{-1}\boldsymbol{\Xi}_i\Big)^{-1}\boldsymbol{\Xi}_i{}^T\boldsymbol{\Sigma}^{-1}\mathbf{x}. \end{aligned} \tag{17}$$

This R_i is the directional PCA or diPCA monitoring statistic. Note that

$$\big[\boldsymbol{U}, \widetilde{\boldsymbol{U}}\big]\big[\boldsymbol{U}, \widetilde{\boldsymbol{U}}\big]^T = \boldsymbol{U}\boldsymbol{U}^T + \widetilde{\boldsymbol{U}}\widetilde{\boldsymbol{U}}^T = \mathbf{I}_p \tag{18}$$

$$\boldsymbol{\Sigma}^{-1} = \big(\boldsymbol{A}\boldsymbol{A}^T + \sigma\mathbf{I}_p\big)^{-1} = \frac{1}{\sigma}\Big(\mathbf{I}_p - \boldsymbol{A}\big(\boldsymbol{A}^T\boldsymbol{A} + \sigma\mathbf{I}_q\big)^{-1}\boldsymbol{A}^T\Big). \tag{19}$$

Combined with (10), there is

$$\boldsymbol{\Sigma}^{-1} = \boldsymbol{U}\boldsymbol{\Lambda}_q^{-1}\boldsymbol{U}^T + \frac{1}{\sigma}\big(\mathbf{I}_p - \boldsymbol{U}\boldsymbol{U}^T\big). \tag{20}$$

By noting (20), T^2 in (5), and Q in (6), it turns out that many known monitoring statistics are special cases of the diPCA statistic (17) with appropriate choices of the fault direction matrix $\boldsymbol{\Xi}_i$. To be specific,

1) with $\boldsymbol{\Xi}_i = \boldsymbol{U}$, indicating that faults have occurred in the principal component subspace, the statistic (17) becomes

Hotelling's T^2 statistic, specialized for detecting process faults;

2) with $\boldsymbol{\Xi}_i = \widetilde{\boldsymbol{U}}$, indicating that faults have occurred in the residual subspace, the statistic (17) becomes the Q statistic up to a multiplier $1/\sigma$;
3) with $\boldsymbol{\Xi}_i = \mathbf{I}_p$, indicating general faults, the statistic (17) becomes a new combined index

$$W = \mathbf{x}^T \boldsymbol{\Sigma}^{-1} \mathbf{x} = T^2 + \frac{1}{\sigma} Q. \tag{21}$$

Unlike the conventional combined index (7) that still relies on the choice of an extra parameter α, such as α in J_{α,T^2}, this LRT-based combined index (21) is a natural and unique result of LRT, with theoretically sound foundations. By noting the two coefficients associated with T^2 and Q in (21) are 1 and $(1/\sigma)$, respectively, in proportion to σ:1, the LRT actually tells us that in combining the two statistics T^2 and Q, an optimal proportion between them is σ:1, where σ is calculated based on (11), the average of the remaining eigenvalues $\lambda_{q+1}, \ldots, \lambda_p$. The T_c^2 statistic in [23, eq. (23)] is actually the combined index (21), but [23] does not reveal that T_c^2 is the combination of T^2 and Q, unfortunately. In [27], T^2 and $(1/\sigma)Q$ were also derived from the PPCA model in a different way, but they were not added to form a combined statistic. Hereafter, the monitoring approach in (21) is referred to as "PPCA," since it is derived from the PPCA model with $\boldsymbol{\Xi}_i = \mathbf{I}_p$.

By denoting

$$\mathbf{t} = \left[\boldsymbol{U}, \widetilde{\boldsymbol{U}}\right]^T \mathbf{x} \tag{22}$$

in a similar manner to [9], T^2, $(1/\sigma)Q$, the combined statistic in (7), the Mahalanobis distance (the global Hotelling's T^2)

$$D^2 = \mathbf{x}^T \boldsymbol{\Omega}^{-1} \mathbf{x} \tag{23}$$

in [9], and the PPCA statistic in (21) can be summarized as the quadratic form $\mathbf{t}^T \boldsymbol{\Phi} \mathbf{t}$, with

$$\boldsymbol{\Phi} = \begin{cases} \operatorname{diag}\left\{\lambda_1^{-1}, \ldots, \lambda_q^{-1}, \underbrace{0, \ldots, 0}_{p-q}\right\}, & \text{for } T^2 \\ \operatorname{diag}\left\{\underbrace{0, \ldots, 0}_{q}, \underbrace{\sigma^{-1}, \ldots, \sigma^{-1}}_{p-q}\right\}, & \text{for } \frac{1}{\sigma} Q \\ \operatorname{diag}\left\{\lambda_1^{-1} J_{\alpha,T^2}^{-1}, \ldots, \lambda_q^{-1} J_{\alpha,T^2}^{-1}, \right. & \\ \qquad \left. \underbrace{J_{\alpha,Q}^{-1}, \ldots, J_{\alpha,T^2}^{-1}}_{p-q}\right\}, & \text{for combined} \\ \operatorname{diag}\left\{\lambda_1^{-1}, \ldots, \lambda_q^{-1}, \lambda_{q+1}^{-1}, \ldots, \lambda_p^{-1}\right\}, & \text{for } D^2 \\ \operatorname{diag}\left\{\lambda_1^{-1}, \ldots, \lambda_q^{-1}, \underbrace{\sigma^{-1}, \ldots, \sigma^{-1}}_{p-q}\right\}, & \text{for PPCA.} \end{cases} \tag{24}$$

In particular, the Mahalanobis distance statistic D^2 in (23) involves the inverses of the remaining very small eigenvalues $\lambda_{q+1}, \ldots, \lambda_p$, and the estimation inaccuracy of $\lambda_{q+1}, \ldots, \lambda_p$ leads to large biases in $\lambda_{q+1}^{-1}, \ldots, \lambda_p^{-1}$. The PPCA monitoring statistic, however, replaces these near-zero eigenvalues with their average, which is σ calculated from (11). Based on (11), it can be seen that σ actually only relies on the q leading eigenvalues $\lambda_1, \ldots, \lambda_q$, which avoids $\lambda_{q+1}^{-1}, \ldots, \lambda_p^{-1}$ in D^2, so the estimation accuracy of σ can be guaranteed. Therefore, compared with D^2, the PPCA monitoring statistic can be used as a combined index with ease.

Furthermore, according to [28, Th. 10.3.3], in the normal operating condition, the quadratic form R_i in (17) follows asymptotically the chi-square distribution $\chi_{r_i}^2$ with r_i degrees of freedom (d.f.), where r_i is the rank of the fault direction matrix $\boldsymbol{\Xi}_i$. This naturally leads to Theorem 1, and its detailed proof can be found in the Appendix.

Theorem 1: In the normal case, $(1/\sigma)Q$ and the PPCA monitoring index W in (21) follow asymptotically the chi-square distributions χ_{p-q}^2 with d.f. $= p - q$ and χ_p^2 with d.f. $= p$, respectively.

As in Theorem 1, T^2 follows asymptotically the chi-square distribution χ_q^2. In fact, Jackson and Mudholkar [19] provided a theoretical control limit of Q, which, however, has a rather complex form. Compared to it, Theorem 1 here leads to a control limit of Q with a fairly concise form based on χ_{p-q}^2.

B. Composite Directional PCA

Hypothesis (13) assumes that the fault direction matrix $\boldsymbol{\Xi}_i$ is known, and the monitoring statistic (17), which is developed from hypothesis (13), can be used for fault detection. But in reality, this is not always the case. The fault may come from another subspace spanned by the columns of matrix $\boldsymbol{\Xi}_j$ of dimension $p \times r_j$, which has orthogonal columns satisfying $\boldsymbol{\Xi}_j^T \boldsymbol{\Xi}_j = \mathbf{I}_{r_j}$ and $\boldsymbol{\Xi}_j^T \boldsymbol{\Xi}_i = \mathbf{0}$ $(j \neq i)$. In general, the fault may be in one of the several mutually orthogonal subspaces formed by the columns of matrices $\boldsymbol{\Xi}_i$ $(i \in \mathcal{F})$, respectively, where $\mathcal{F}$ is the fault set. Therefore, the fault detection problem can be formulated as testing the composite hypothesis

$$H_0 : \boldsymbol{\mu} = \mathbf{0} \quad \text{versus} \quad H_1 : \bigvee_{i \in \mathcal{F}} \boldsymbol{\mu} = \boldsymbol{\Xi}_i \mathbf{f}_i. \tag{25}$$

Here, $\vee$ represents the "XOR" (exclusive or) operation, implying that only one of $\boldsymbol{\mu} = \boldsymbol{\Xi}_i \mathbf{f}_i$ $(i \in \mathcal{F})$ is true. By the matrix theory, the entire fault space can always be decomposed into several mutually orthogonal subspaces spanned by the columns of matrices $\boldsymbol{\Xi}_i$ $(i \in \mathcal{F})$, such as columns of the identity matrix $\mathbf{I}_p$, that is, $\mathbf{e}_i$ $(i = 1, \ldots, p)$, or the eigenvector matrices $\boldsymbol{U}$ and $\widetilde{\boldsymbol{U}}$. These direction matrices are known and mutually orthogonal. Any fault, mathematically speaking, either lies in one of these prespecified mutually orthogonal subspaces, which is stated in hypothesis (25), or can be decomposed into at least two of these subspaces. In either case, the proposed cdiPCA monitoring statistic, developed from hypothesis (25), can be powerful. See Table III for detailed simulation results of this.

Based on the monitoring statistic R_i in (17), the LRT statistic for testing hypothesis (25) should be the maximum among R_i

($i \in \mathcal{F}$), which is

$$R = \max_{i \in \mathcal{F}} \mathbf{x}^T \boldsymbol{\Sigma}^{-1} \boldsymbol{\Xi}_i \left(\boldsymbol{\Xi}_i{}^T \boldsymbol{\Sigma}^{-1} \boldsymbol{\Xi}_i \right)^{-1} \boldsymbol{\Xi}_i{}^T \boldsymbol{\Sigma}^{-1} \mathbf{x}. \tag{26}$$

In fact, the detectability of a fault occurring exactly in the column subspace of matrix $\boldsymbol{\Xi}_i$ is guaranteed by the following theorem.

Theorem 2: If a fault, say fault i, occurs with the fault direction $\boldsymbol{\Xi}_i$, that is, $\boldsymbol{\Xi}_i \mathbf{f}_i$, for any $j \in \mathcal{F}$ and $j \neq i$, with $\mathbf{x} = \boldsymbol{\Xi}_i \mathbf{f}_i$, there is

$$\begin{aligned} &\mathbf{x}^T \boldsymbol{\Sigma}^{-1} \boldsymbol{\Xi}_i \left(\boldsymbol{\Xi}_i{}^T \boldsymbol{\Sigma}^{-1} \boldsymbol{\Xi}_i \right)^{-1} \boldsymbol{\Xi}_i{}^T \boldsymbol{\Sigma}^{-1} \mathbf{x} \\ &\quad \geq \mathbf{x}^T \boldsymbol{\Sigma}^{-1} \boldsymbol{\Xi}_j \left(\boldsymbol{\Xi}_j{}^T \boldsymbol{\Sigma}^{-1} \boldsymbol{\Xi}_j \right)^{-1} \boldsymbol{\Xi}_j{}^T \boldsymbol{\Sigma}^{-1} \mathbf{x}. \end{aligned} \tag{27}$$

The proof can be found in the Appendix.

Recall that in the normal case, R_i in (17) follows asymptotically the chi-square distribution $\chi^2_{r_i}$. However, for each R_i ($i \in \mathcal{F}$), the d.f. r_i of these chi-square distributions are not necessarily identical. Simply taking the maximum among these R_i may lead to misleading results. Before maximizing them, one appropriate solution is to apply some normalization procedure for standardization. To be specific, the cumulative distribution function of $\chi^2_{r_i}$ evaluated at R_i is applied, which transforms the monitoring statistic R_i into a uniformly distributed one lying in the interval $(0, 1)$, that is, the uniform distribution $U(0, 1)$. In other words

$$\max_{i \in \mathcal{F}} \chi^2_{r_i} \left(\mathbf{x}^T \boldsymbol{\Sigma}^{-1} \boldsymbol{\Xi}_i \left(\boldsymbol{\Xi}_i{}^T \boldsymbol{\Sigma}^{-1} \boldsymbol{\Xi}_i \right)^{-1} \boldsymbol{\Xi}_i{}^T \boldsymbol{\Sigma}^{-1} \mathbf{x} \right) \tag{28}$$

should be the monitoring statistic if r_i ($r \in \mathcal{F}$) are not identical.

In a word, given R_i in (17), the cdiPCA monitoring statistic is summarized as

$$R = \begin{cases} \max_{i \in \mathcal{F}} R_i, & \text{if } r_i (i \in \mathcal{F}) \text{ are equal} \\ \max_{i \in \mathcal{F}} \chi^2_{r_i}(R_i), & \text{if } r_i (i \in \mathcal{F}) \text{ are unequal.} \end{cases} \tag{29}$$

As with diPCA, the cdiPCA monitoring statistic also includes some special cases.

First, faults in either the principal subspace or the residual subspace are considered, which leads to the hypothesis

$$\begin{aligned} &H_0 : \boldsymbol{\mu} = \mathbf{0} \quad \text{versus} \\ &H_1 : \boldsymbol{\mu} = \boldsymbol{U}\mathbf{f} \text{ or } \boldsymbol{\mu} = \widetilde{\boldsymbol{U}}\widetilde{\mathbf{f}}. \end{aligned} \tag{30}$$

Notice $\boldsymbol{U}$ of dimension $p \times q$ and $\widetilde{\boldsymbol{U}}$ of dimension $p \times (p-q)$, where q is the number of principal components. According to the cdiPCA scheme in (29), after some simplifications, there is the following monitoring statistic:

$$\max \left\{ \chi^2_q \left(T^2 \right), \chi^2_{p-q} \left(\frac{1}{\sigma} Q \right) \right\}. \tag{31}$$

In fact, this statistic is equivalent to the T^2-Q scheme mentioned in Section II-A.

So far, it has been shown that the existing monitoring statistics T^2, Q, and T^2-Q, as well as the proposed PPCA statistic W in (21) are derived from the (composite) diPCA framework. It should be highlighted that diPCA can incorporate fault directions into alternative hypotheses and derive monitoring statistics that speed fault detection.

Furthermore, as in [14], assume that there is at most one sensor fault, say in the ith sensor. This is common in practice since faults tend to occur in only a few components, namely, sparsity. In this case, the fault is expressed as $\mathbf{e}_i f_i$, where the $p \times 1$ fault direction vector $\mathbf{e}_i$ has 1 in its ith element and 0 elsewhere, and f_i is the fault magnitude. In general, however, the fault location i is still unknown, namely, $i = 1$ or $\ldots$ or p. Therefore, monitoring such directional sensor faults is equivalent to testing the hypothesis

$$H_0 : \boldsymbol{\mu} = \mathbf{0} \quad \text{versus} \quad H_1 : \bigvee_{i \in \{1, \ldots, p\}} \boldsymbol{\mu} = \mathbf{e}_i f_i. \tag{32}$$

This is like hypothesis (25), and note that the direction matrices $\boldsymbol{\Xi}_i = \mathbf{e}_i$ all have rank 1 here. As a result, based on the cdiPCA scheme in (29), the monitoring statistic for testing the above hypothesis is

$$S = \max_{i \in \{1, \ldots, p\}} S_i = \max_{i \in \{1, \ldots, p\}} \frac{\left(\mathbf{e}_i^T \boldsymbol{\Sigma}^{-1} \mathbf{x} \right)^2}{\mathbf{e}_i^T \boldsymbol{\Sigma}^{-1} \mathbf{e}_i}. \tag{33}$$

The expression of $\boldsymbol{\Sigma}^{-1}$ can be found in (20). This statistic focuses on monitoring directional sensor faults, namely, faults occurring at only one senor. Since it incorporates such directional fault information, its detection power for sparse sensor faults can be anticipated. The monitoring statistic in (33) is referred to as "cdiPCA."

In addition, S_i in (33) follows asymptotically χ^2_1 and, therefore, S in (33) follows asymptotically the distribution of the maximum of p χ^2_1 distributed variables that are not necessarily independent. This makes it difficult to determine the theoretical control limit of S. Therefore, the focus is not on its exact control limit. Instead, the Monte Carlo simulations are employed to determine this limit such that the significance level or the type I error probability achieves a specified value. The simulated and theoretical values of these control limits are also compared later.

C. Directional-PCA-Based Diagnosis

The cdiPCA monitoring statistic in (29) also facilitates fault diagnosis. To be specific, let $\mathbf{y}$ be the observation vector that triggers an alarm. The fault ζ should be diagnosed as

$$\hat{\zeta} = \begin{cases} \arg\max_{i \in \mathcal{F}} R_i, & \text{if } r_i (i \in \mathcal{F}) \text{ are equal} \\ \arg\max_{i \in \mathcal{F}} \chi^2_{r_i}(R_i), & \text{if } r_i (i \in \mathcal{F}) \text{ are unequal} \end{cases} \tag{34}$$

with

$$R_i = \mathbf{y}^T \boldsymbol{\Sigma}^{-1} \boldsymbol{\Xi}_i \left(\boldsymbol{\Xi}_i{}^T \boldsymbol{\Sigma}^{-1} \boldsymbol{\Xi}_i \right)^{-1} \boldsymbol{\Xi}_i{}^T \boldsymbol{\Sigma}^{-1} \mathbf{y}. \tag{35}$$

Furthermore, the fault magnitude can be estimated or reconstructed as

$$\widehat{\mathbf{f}}_{\hat{\zeta}} = \left(\boldsymbol{\Xi}_{\hat{\zeta}}{}^T \boldsymbol{\Sigma}^{-1} \boldsymbol{\Xi}_{\hat{\zeta}} \right)^{-1} \boldsymbol{\Xi}_{\hat{\zeta}}{}^T \boldsymbol{\Sigma}^{-1} \mathbf{y}. \tag{36}$$

The diagnostic method in (34) can be applied to the T^2-Q monitoring scheme, identifying whether the fault is in the principal component subspace or in the residual subspace. This is completed by comparing $\chi^2_q(T^2)$ and $\chi^2_{p-q}([1/\sigma]Q)$.

In addition, it can also be applied to the cdiPCA monitoring method, which gives rise to the sensor fault

$$\hat{\zeta} = \arg \max_{i \in \{1,\ldots,p\}} \frac{\left(\mathbf{e}_i^T \boldsymbol{\Sigma}^{-1} \mathbf{y}\right)^2}{\mathbf{e}_i^T \boldsymbol{\Sigma}^{-1} \mathbf{e}_i}. \tag{37}$$

Moreover, the fault magnitude is reconstructed as

$$\hat{f}_{\hat{\zeta}} = \frac{\mathbf{e}_{\hat{\zeta}}^T \boldsymbol{\Sigma}^{-1} \mathbf{y}}{\mathbf{e}_{\hat{\zeta}}^T \boldsymbol{\Sigma}^{-1} \mathbf{e}_{\hat{\zeta}}}. \tag{38}$$

For process diagnosis, Alcala and Qin proposed an RBC method and showed that it had better performance for fault diagnosis than the conventional contribution plot methods [14]. The RBC method first reconstructs the fault magnitude along each possible fault direction and then computes the contribution indices of the directions. The direction with the maximum contribution is recognized to be the fault direction. Specifically, with the combined monitoring statistic (7), this RBC scheme for diagnosis is expressed as

$$\hat{\zeta} = \arg \max_{i \in \{1,\ldots,p\}} \frac{\left(\mathbf{e}_i^T \mathbf{M} \mathbf{y}\right)^2}{\mathbf{e}_i^T \mathbf{M} \mathbf{e}_i} \tag{39}$$

with

$$\mathbf{M} = \frac{1}{J_{\alpha,T^2}} \boldsymbol{U} \boldsymbol{\Lambda}_q^{-1} \boldsymbol{U}^T + \frac{1}{J_{\alpha,Q}} \widetilde{\boldsymbol{U}} \widetilde{\boldsymbol{U}}^T. \tag{40}$$

Matrix $\mathbf{M}$ can also be other choices, such as $\boldsymbol{U} \boldsymbol{\Lambda}_q^{-1} \boldsymbol{U}^T$ and $\widetilde{\boldsymbol{U}} \widetilde{\boldsymbol{U}}^T$ [14]. If $\mathbf{M} = \boldsymbol{\Sigma}^{-1}$ is taken, this RBC scheme coincides with the proposed diagnostic scheme (37). Therefore, the diagnostic scheme (37) can be regarded as a type of RBC methods, which, however, stems from the diPCA framework.

IV. Performance Assessment

A. Comparison Criteria

In this section, the performance of the proposed PPCA statistic (21) and the cdiPCA statistic (33) is investigated and compared with the conventional T^2-Q scheme and the combined index (7). For fairness, the type I error probabilities or significance levels of all the four approaches are set at $\alpha = 0.005$. In particular, the T^2-Q scheme is actually composed of two separate monitoring statistics T^2 and Q, and triggers an alarm whenever there is a signal from at least one of them. In order to keep the overall type I error probability α of the T^2-Q scheme, T^2 and Q can be set both with an individual type I error probability $\alpha' = 1 - (1-\alpha)^{[1/2]} = 0.002503$.

Furthermore, as a convention in statistical process control, the ARL is used to measure the performance of a monitoring scheme, which measures on average the lengths before an alarm is triggered. Usually, a single run is actually a random number because of process randomness and, therefore, a comparison based only on a single run does not make much sense. For thorough investigation, here 10 000 replicated simulations are performed, that is, 10 000 runs to compute one ARL.

In terms of ARLs, in the normal case, the ARL is denoted by ARL_0, which corresponds to the type I error probability α and is equal to $1/\alpha = 200$. This follows because, given the probability that a monitoring statistic falls beyond its control limit, the run length follows a geometric distribution with this probability. Therefore, ARL_0 is the mean of the geometric distribution $\text{Geo}(\alpha)$. In fact, α is also the false alarm rate, the probability of triggering an alarm in normal operation. In particular, ARL_0s of the T^2 and Q statistics in the T^2-Q scheme should be $1/\alpha' = 399.5$, such that the joint ARL_0 is 200. For the combined index (7), αs in the involved two denominators J_{α,T^2} and $J_{\alpha,Q}$ are chosen as 0.005, but they may take other values, say 0.002.

In the faulty state, ARL_1 is used to measure the detection performance of a monitoring method. Here, ARL_1 is equal to $1/(1-\beta)$, where β is the type II error probability or the missing alarm rate, the probability of failing to trigger an alarm when the process is faulty. When a fault occurs, with the same ARL_0, a method with a smaller ARL_1 indicates that it detects this fault faster and outperforms others.

B. Determining Control Limits

As mentioned previously, under normal operating conditions, T^2, $(1/\sigma)Q$, PPCA statistics follow asymptotically the chi-square distributions χ_q^2, χ_{p-q}^2, and χ_p^2, respectively. In addition, the cdiPCA statistic (33) is the maximum of the p χ_1^2 distributed variables that are not necessarily independent, and [17] provided the theoretical control limit of the combined statistic (7). In addition to theoretical control limits, bisection and Monte Carlo simulations are employed here to determine them. The procedures are as follows.

1) Set a and b as the initial lower and upper bounds, respectively.
2) Use the midpoint $c = 0.5(a+b)$ as the control limit for simulations and obtain the corresponding ARL_0.
3) If the above $\text{ARL}_0 - 200 < -\gamma$, set $a = c$; if the above $\text{ARL}_0 - 200 > \gamma$, set $b = c$. Here, $\gamma > 0$ is a prespecified precision, usually selected as the one standard error, that is, the standard deviation of run lengths$/\sqrt{N} \approx 200/\sqrt{N}$, with $N = 10\,000$ being the number of replicated simulations and therefore $\gamma = 2$ here. Repeat the above procedures until $|\text{ARL}_0 - 200| < \gamma$.

Consider the normal-case model

$$\mathbf{x} = \boldsymbol{A}\mathbf{z} + \boldsymbol{\epsilon} \text{ with } \mathbf{z} \sim \text{N}(\mathbf{0}; \mathbf{I}_3) \text{ and } \boldsymbol{\epsilon} \sim \text{N}(\mathbf{0}; \sigma \mathbf{I}_6) \tag{41}$$

and

$$\boldsymbol{A} = 5 \times \begin{bmatrix} 0.525 & 0.175 & -0.068 \\ 0.126 & -0.152 & 0.558 \\ 0.245 & 0.216 & 0.481 \\ 0.112 & 0.167 & 0.387 \\ 0.346 & 0.535 & -0.053 \\ 0.132 & -0.211 & 0.462 \end{bmatrix}, \ \sigma = 0.25. \tag{42}$$

Based on this model, the original covariance matrix $\boldsymbol{\Omega}$ can be calculated. By performing the eigenvalue decomposition of $\boldsymbol{\Omega}$, based on the CPV criterion, $q = 3$ principal components are obtained; whereas, the original dimension $p = 6$. The link matrix $\boldsymbol{A}$ and the sensor error variance σ are estimated using (10) and (11), respectively.

To see the effectiveness of simulation methods in determining control limits, their theoretical and simulated limits for the

TABLE I
COMPARISON OF THEORETICAL AND SIMULATED CONTROL LIMITS

	T^2-Q			combined	PPCA	cdiPCA
theoretical	14.3178	3.6188	3.5795	1.4401	18.5476	12.4472
simulated	14.3100	3.5775		1.4406	18.5400	11.0000

four methods are listed in Table I, denoted by T^2-Q, combined, PPCA, cdiPCA, respectively. In particular, there are two control limits for the T^2-Q scheme, one for T^2 and the other for Q. Note that there are two methods to calculate the theoretical control limit of Q. One is 3.6188, calculated from [19], and the other is 3.5795, which follows because $(1/\sigma)Q$ is asymptotically subject to χ^2_3. The latter is simple to calculate and very close to the simulated value 3.5775. Throughout Table I, it is shown that for the T^2-Q scheme, the combined index (7), and the PPCA statistic (21), their theoretical and simulated control limits are very close. This demonstrates the effectiveness of simulation methods.

However, there seems to be large deviation between the theoretical and simulated values for the cdiPCA statistic (33). This follows because the theoretical value is based on the independent assumption of S_i in (33) for different $i = 1, \ldots, 6$, which is not necessarily the case in reality. To be specific, this value is calculated using the following approximation [29]:

$$c_p\big(R_t - d_p\big) \xrightarrow{d} \Psi \tag{43}$$

where $\xrightarrow{d}$ means convergence in distribution, Ψ follows the Gumbel distribution with the cumulative distribution function $\Pr(\Psi \le x) = e^{-e^{-x}}$ and the quantile function $-\ln(-\ln\alpha)$, and $c_p = (1/2)$, $d_p = 2\ln p - \ln\ln p - \ln\pi = 2\ln 6 - \ln\ln 6 - \ln\pi = 1.8556$. With the Type I error probability $\alpha = 0.005$, the quantile of the Gumbel distribution is 5.2958, and finally, the theoretical value of the control limit of the cdiPCA statistic (33) is $5.2958/c_p + d_p = 12.4472$. See also [29, Table 3.4.4] for the detailed derivation to approximate the quantile of p independent chi-square distributions.

C. Comparison in Process Monitoring

The performance of the four methods: 1) T^2-Q; 2) combined; 3) PPCA; and 4) cdiPCA in detecting single-sensor faults is studied, where the fault occurs in a single unknown sensor, say the ith ($i = 1$ or , $\ldots$, or 6), with magnitude f_i. The results for comparison are obtained by Monte Carlo simulations based on model (41) with the parameter settings in (42) and are displayed in Table II. Note that the standard errors of ARL_1s are also reported in parentheses, facilitating comparison. Note that $\text{ARL}_0 = 200$ in the fault-free case. In all six cases (f_1–f_6), as the fault magnitude increases (in absolute value), the ARL_1s resulting from each approach decrease. For instance, the PPCA index in (21) has a large ARL_1 100 for $f_1 = -1.0$ and a small ARL_1 2.95 for $f_1 = -4.0$. Specifically, PPCA slightly outperforms the combined index (7) by approximately one standard error. This advantage holds uniformly throughout Table II and is because of the power of LRT. Also, except f_1, T^2-Q detects large faults faster but small faults slower than combined and PPCA.

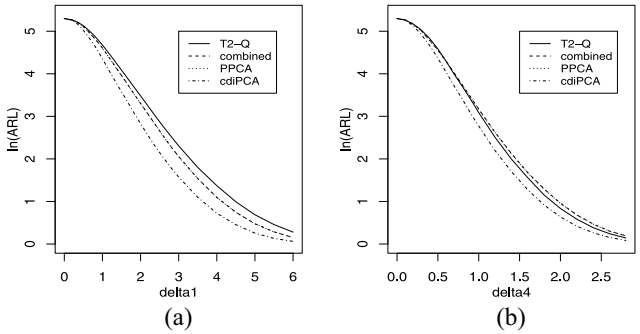

Fig. 1. ARL curves of the four methods in detecting single-sensor faults. (a) Sensor 1. (b) Sensor 4.

In addition, Table II shows that for all the faults f_1–f_6, the cdiPCA method, namely, cdiPCA in (33), has uniformly smaller ARL_1s (the best results are in bold) and, therefore, detects all the single-sensor faults uniformly much faster than all the other three methods, and this superiority is significant. It follows because cdiPCA narrows down to single-sensor faults alone, and its test power has been improved to a large extent. This verifies that incorporating such directional information facilitates fault detection, but such information is completely ignored by conventional PCA-based process monitoring approaches, such as T^2-Q and combined.

To investigate the performance of the four methods thoroughly, curves are also drawn to display how ARL_1s change with fault magnitudes f_1 and f_4 for sensors 1 and 4, respectively, in Fig. 1. It shows that the cdiPCA statistic (33) uniformly has the shortest ARL_1s and stands out by a large margin.

Furthermore, multiple-sensor faults are considered. Suppose that sensors 1 and 4 are known to be faulty in advance and, therefore, the fault direction matrix should be $\boldsymbol{\Xi}_i = [\mathbf{e}_1, \mathbf{e}_4]$. Based on (17), a monitoring statistic can be developed, denoted by diPCA. Here, the investigation of diPCA in (17) actually shows the advantage of knowing the fault direction matrix, which, however, may be unknown in practice. It is assumed that both sensor faults have magnitude $f_{1,4}$. The comparison results between T^2-Q, combined, PPCA, cdiPCA, and diPCA are listed in the upper half of Table III. Similarly, it is also assumed that sensors 2, 3, and 6 are faulty with the fault direction matrix $\boldsymbol{\Xi}_i = [\mathbf{e}_2, \mathbf{e}_3, \mathbf{e}_6]$ and all with magnitude $f_{2,3,6}$. The comparison results are listed in the lower half of Table III. Here, to set $\text{ARL}_0 = 200$, the control limits can also be determined by simulations, which are approximately equal to their theoretical values, namely, the quantiles of the chi-square distributions χ^2_2 or χ^2_3 (like Theorem 1).

According to Table III, by exploiting the fault directions fully, the diPCA statistic that assumes known direction matrices uniformly outperforms the other four approaches in all cases, showing the advantage of the diPCA monitoring scheme (17). In addition, it is noteworthy that cdiPCA still outperforms and detects faults earlier than T^2-Q, combined, and PPCA with smaller ARL_1s, although the true fault direction matrices $[\mathbf{e}_1, \mathbf{e}_4]$ and $[\mathbf{e}_2, \mathbf{e}_3, \mathbf{e}_6]$ violate the assumption in hypothesis (25).

TABLE II
ARL COMPARISON IN DETECTING SINGLE-SENSOR FAULTS

f_1	T^2-Q		combined		PPCA		cdiPCA	
−4.0	3.82	(0.03)	2.97	(0.02)	2.95	(0.02)	**2.06**	(0.01)
−2.0	32.2	(0.32)	27.1	(0.27)	26.9	(0.26)	**16.8**	(0.16)
−1.0	107	(1.07)	101	(1.00)	100	(0.99)	**77.3**	(0.77)
1.0	107	(1.06)	100	(0.99)	99.3	(0.99)	**77.8**	(0.76)
2.0	32.5	(0.32)	27.3	(0.27)	27.0	(0.26)	**16.9**	(0.16)
4.0	3.94	(0.03)	2.99	(0.02)	2.98	(0.02)	**2.06**	(0.01)
f_2	T^2-Q		combined		PPCA		cdiPCA	
−2.0	2.75	(0.02)	3.20	(0.03)	3.17	(0.03)	**2.22**	(0.02)
−1.0	26.5	(0.26)	28.4	(0.29)	28.1	(0.28)	**19.4**	(0.19)
−0.5	105	(1.05)	104	(1.05)	103	(1.04)	**87.5**	(0.87)
0.5	104	(1.03)	104	(1.02)	103	(1.01)	**84.8**	(0.84)
1.0	26.4	(0.26)	28.6	(0.28)	28.3	(0.28)	**19.4**	(0.19)
2.0	2.77	(0.02)	3.20	(0.02)	3.17	(0.02)	**2.25**	(0.02)
f_3	T^2-Q		combined		PPCA		cdiPCA	
−2.0	2.79	(0.02)	3.20	(0.03)	3.17	(0.03)	**2.26**	(0.02)
−1.0	26.8	(0.26)	28.3	(0.28)	28.0	(0.28)	**19.1**	(0.19)
−0.5	105	(1.04)	104	(1.04)	103	(1.03)	**86.7**	(0.88)
0.5	105	(1.03)	102	(1.01)	101	(1.00)	**86.9**	(0.87)
1.0	26.8	(0.27)	28.8	(0.29)	28.5	(0.28)	**19.4**	(0.19)
2.0	2.84	(0.02)	3.27	(0.03)	3.25	(0.03)	**2.26**	(0.02)
f_4	T^2-Q		combined		PPCA		cdiPCA	
−2.0	2.30	(0.02)	2.62	(0.02)	2.60	(0.02)	**1.89**	(0.01)
−1.0	22.1	(0.22)	23.9	(0.23)	23.6	(0.23)	**15.9**	(0.15)
−0.5	97.1	(0.98)	94.7	(0.93)	93.6	(0.91)	**77.6**	(0.77)
0.5	97.9	(0.97)	95.3	(0.95)	94.5	(0.94)	**78.7**	(0.77)
1.0	21.9	(0.21)	23.8	(0.23)	23.6	(0.23)	**16.0**	(0.15)
2.0	2.30	(0.02)	2.61	(0.02)	2.59	(0.02)	**1.89**	(0.01)
f_5	T^2-Q		combined		PPCA		cdiPCA	
−2.0	6.27	(0.06)	6.90	(0.06)	6.85	(0.06)	**4.20**	(0.04)
−1.0	48.4	(0.48)	48.9	(0.49)	48.5	(0.48)	**30.6**	(0.30)
−0.5	132	(1.31)	129	(1.29)	128	(1.28)	**101**	(1.01)
0.5	131	(1.29)	130	(1.28)	129	(1.27)	**101**	(1.00)
1.0	48.7	(0.49)	49.1	(0.49)	48.7	(0.48)	**30.9**	(0.30)
2.0	6.09	(0.06)	6.86	(0.06)	6.77	(0.06)	**4.09**	(0.04)
f_6	T^2-Q		combined		PPCA		cdiPCA	
−2.0	2.84	(0.02)	3.24	(0.03)	3.21	(0.03)	**2.26**	(0.02)
−1.0	26.8	(0.26)	28.8	(0.28)	28.5	(0.28)	**18.8**	(0.18)
−0.5	105	(1.04)	103	(1.02)	102	(1.00)	**83.1**	(0.82)
0.5	105	(1.04)	103	(1.02)	103	(1.01)	**83.5**	(0.83)
1.0	26.7	(0.26)	28.9	(0.28)	28.5	(0.28)	**18.6**	(0.18)
2.0	2.76	(0.02)	3.10	(0.03)	3.08	(0.03)	**2.18**	(0.02)

Note: standard errors are in parentheses. The best results are in bold.

TABLE III
ARL COMPARISON IN DETECTING MULTIPLE-SENSOR FAULTS

$f_{1,4}$	T^2-Q		combined		PPCA		cdiPCA		diPCA	
−2.0	1.25	(0.01)	1.34	(0.01)	1.33	(0.01)	1.18	(0.00)	**1.14**	(0.00)
−1.0	9.25	(0.09)	10.6	(0.10)	10.5	(0.10)	6.70	(0.06)	**4.71**	(0.04)
−0.5	62.6	(0.62)	63.0	(0.63)	62.3	(0.62)	45.0	(0.44)	**22.0**	(0.22)
−0.2	161	(1.59)	158	(1.57)	158	(1.56)	142	(1.43)	**54.5**	(0.55)
0.2	162	(1.60)	160	(1.61)	159	(1.60)	144	(1.43)	**54.6**	(0.54)
0.5	62.3	(0.61)	63.5	(0.63)	62.8	(0.62)	44.9	(0.45)	**21.8**	(0.21)
1.0	9.23	(0.09)	10.6	(0.10)	10.5	(0.10)	6.83	(0.06)	**4.81**	(0.04)
2.0	1.26	(0.01)	1.35	(0.01)	1.35	(0.01)	1.18	(0.00)	**1.15**	(0.00)
$f_{2,3,6}$	T^2-Q		combined		PPCA		cdiPCA		diPCA	
−2.0	5.06	(0.05)	5.39	(0.05)	5.35	(0.05)	4.22	(0.04)	**3.55**	(0.03)
−1.0	42.0	(0.41)	41.8	(0.41)	41.4	(0.41)	32.5	(0.32)	**26.9**	(0.26)
−0.5	125	(1.24)	119	(1.19)	119	(1.19)	108	(1.08)	**96.5**	(0.94)
−0.2	183	(1.83)	183	(1.83)	182	(1.82)	180	(1.79)	**173**	(1.74)
0.2	183	(1.83)	183	(1.82)	182	(1.80)	178	(1.79)	**174**	(1.73)
0.5	124	(1.23)	120	(1.19)	119	(1.18)	107	(1.08)	**96.8**	(0.97)
1.0	41.8	(0.41)	41.8	(0.41)	41.4	(0.41)	32.8	(0.33)	**27.0**	(0.27)
2.0	5.02	(0.05)	5.39	(0.05)	5.34	(0.05)	4.15	(0.04)	**3.51**	(0.03)

NOTE: Standard errors are in parentheses. The best results are in bold.

TABLE IV
MATCHING RATES (%) COMPARISON IN DIAGNOSING SINGLE-SENSOR FAULTS

f_1	RBC	cdiPCA	f_4	RBC	cdiPCA
−4.0	**83.28**	83.24	−2.0	**94.78**	**94.78**
−2.0	63.39	**63.40**	−1.0	77.82	**77.83**
−1.0	39.91	**39.93**	−0.5	49.21	**49.22**
1.0	**39.70**	39.69	0.5	48.95	**48.96**
2.0	62.88	**62.89**	1.0	78.00	**78.02**
4.0	**84.34**	**84.34**	2.0	94.56	**94.58**
f_2	RBC	cdiPCA	f_5	RBC	cdiPCA
−2.0	**93.39**	**93.39**	−2.0	**73.83**	**73.83**
−1.0	**75.83**	75.82	−1.0	49.74	**49.75**
−0.5	47.02	**47.03**	−0.5	30.43	**30.44**
0.5	**47.81**	**47.81**	0.5	30.83	**30.84**
1.0	74.11	**74.12**	1.0	50.60	**50.62**
2.0	**93.19**	**93.19**	2.0	**74.09**	**74.09**
f_3	RBC	cdiPCA	f_6	RBC	cdiPCA
−2.0	93.37	**93.39**	−2.0	**91.41**	91.40
−1.0	**74.96**	**74.96**	−1.0	**72.64**	72.63
−0.5	**46.73**	**46.73**	−0.5	45.44	**45.45**
0.5	**46.20**	**46.20**	0.5	**43.36**	**43.36**
1.0	**74.80**	74.79	1.0	**71.05**	**71.05**
2.0	**93.33**	93.31	2.0	**91.98**	91.97

NOTE: The best results are in bold.

D. Comparison in Process Diagnosis

Here, the performance of the diagnostic approach (37) derived from cdiPCA is investigated and compared with the RBC scheme (39) proposed by Alcala and Qin [14]. The simulation settings are the same as Table II with unknown single-sensor faults. The observation vector $\mathbf{y}$ used in (37) and (39) is the one that triggers an alarm using the cdiPCA statistic (33). The diagnostic performance is measured by the matching rates that the identified sensor fault is the true fault, and still, this rate is computed based on 10 000 replicated simulations.

The comparison results for diagnosing single-sensor faults are listed in Table IV. It is seen that both diagnostic schemes behave very similarly and that as the fault magnitude increases, the matching rate approaches 100%, regardless of positive or negative faults. However, in terms of the number of best results that are in bold (28 for cdiPCA and 20 for RBC) in Table IV, cdiPCA seems to exhibit a slight advantage over RBC.

TABLE V
F-MEASURE COMPARISON IN THE TE PROCESS

Fault	T^2-Q	combined	ICA	DPCA	I-MPPCA	PPCA	cdiPCA
1	0.9895	0.9944	**0.9988**	0.9981	0.9981	0.9932	0.9804
2	0.9811	**0.9931**	0.9893	0.9893	0.9918	0.9925	0.9708
3	0.1952	0.1471	0.0149	0.0367	0.0344	0.1933	**0.2704**
4	0.9950	0.9975	**1.0000**	0.9981	0.9994	0.9963	0.9877
5	0.7492	0.6396	**1.0000**	0.5208	0.4431	0.7104	0.9833
6	0.9969	0.9994	**1.0000**	0.9988	**1.0000**	0.9988	0.9816
7	0.7353	0.9988	**1.0000**	0.9975	**1.0000**	0.9981	0.9913
8	0.9354	0.9849	**0.9880**	0.9867	**0.9880**	0.9843	0.9529
9	0.1533	0.1136	0.0124	0.0173	0.0149	0.1301	**0.2792**
10	0.7868	0.7909	**0.9116**	0.6190	0.6694	0.8127	0.7877
11	0.8533	0.9171	0.8151	**0.9516**	0.8481	0.9181	0.9159
12	0.9631	0.9937	**0.9988**	0.9925	0.9931	0.9925	0.9660
13	**0.9771**	0.9770	0.9737	0.9757	0.9757	0.9758	0.9692
14	0.9654	0.9981	**1.0000**	0.9981	0.9994	0.9969	0.9846
15	0.2377	0.1853	0.0271	0.0342	0.0368	0.2190	**0.3016**
16	0.7807	0.7628	**0.9342**	0.6237	0.6133	0.7829	0.7965
17	0.9800	0.9842	0.9763	**0.9867**	0.9809	0.9830	0.9709
18	0.9473	0.9459	0.9460	**0.9483**	0.9474	0.9467	0.9458
19	0.7112	0.7099	**0.9153**	0.5953	0.3573	0.7453	0.8297
20	0.8053	0.8053	**0.9419**	0.7007	0.7292	0.8196	0.8110
21	**0.7766**	0.7556	0.6195	0.5990	0.6611	0.7596	0.7593

NOTE: The best results are in bold.

V. CASE STUDY

The TE process is a well-known benchmark dataset for evaluating various fault detection and diagnosis methods, and many papers have employed it for a practical implementation [30], [31]. This dataset involves 41 measured variables that consist of 22 process variables sampled every 3 min and 19 quality variables sampled with time delays, as well as 11 manipulated variables. Here, simultaneously monitoring the 22 process variables XMEAS(1), ..., XMEAS(22) and the 11 manipulated variables XMV(1), ..., XMV(11) is considered; hence, the dimension $p = 33$.

The normal-case training data are first scaled to zero mean and unit variance in each dimension, resulting in the covariance matrix $\mathbf{\Omega}$. By performing PCA on $\mathbf{\Omega}$, $q = 19$ principal components are chosen such that the CPV is larger than 95%, and correspondingly $\boldsymbol{U}$, $\widetilde{\boldsymbol{U}}$, and $\mathbf{\Lambda}_q$ are obtained. In addition, the link matrix $\boldsymbol{A}$ and the sensor error variance $\sigma = 0.0967$ are estimated using (10) and (11), respectively. Until now, all four monitoring methods, that is: 1) the T^2-Q; 2) combined in (7); 3) PPCA in (21); and 4) cdiPCA in (33) can be devised. Their control limits are still chosen by simulations, such that their ARL_0s are all 200, or equivalently with the Type I error probability 0.005. In addition, the improved mixture of PPCA (I-MPPCA) scheme with six local models suggested by Zhang *et al.* [23], the dynamic PCA (DPCA) and independent component analysis (ICA)-based monitoring schemes are all employed here, whose control limits are determined by kernel density estimation to achieve the Type I error probability 0.005.

TABLE VI
F-MEASURE COMPARISON IN THE TE PROCESS FOR FAULTS 5 AND 19

Fault	T^2-Q	combined	ICA	DPCA	I-MPPCA	PPCA	cdiPCA	diPCA
5	0.7492	0.6396	1.0000	0.5208	0.4431	0.7104	0.9833	**0.9822**
19	0.7112	0.7099	0.9153	0.5953	0.3573	0.7453	0.8297	**0.7699**

There are in total 21 faults in the TE process, 160 normal vectors, and 800 faulty vectors in each fault dataset. As recommended by one reviewer, the performance is measured by the F-measure, which considers simultaneously the numbers of false alarms (false positive, FP), true alarms (true positive, TP), and missing alarms (false negative, FN), and it is defined as

$$F = \frac{2\text{TP}}{2\text{TP} + \text{FP} + \text{FN}}. \tag{44}$$

The comparison results are listed in Table V. For Faults 1, 2, 4, 6—8, 11—14, 17, 18, and 21, the proposed PPCA and cdiPCA behave slightly worse than the best approaches (indicated in bold). For Fault 5, cdiPCA is still slightly worse than the best. While ICA has the best performance in detecting Faults 10, 16, 19, and 20, the proposed PPCA and, especially cdiPCA behave best in detecting Faults 3, 9, and 15, where many other approaches, including ICA, are not effective with very small F-measures. This phenomenon was also reported by Dong and Qin [30] and Yin *et al.* [31].

It should be highlighted that in detecting Faults 5 and 19, cdiPCA outperforms PPCA by a large margin. This indicates that the two faults are very likely to be single-sensor faults, where the fault occurs in only one sensor. Thus, the diPCA monitoring statistic in (17) is further employed with the direction matrices using the diagnostic procedure in (37). In fact, we found that of 793 (99.13%) true alarms when detecting Fault 5, (37) attributes 515 alarms to sensor 33, that is, XMV(11). Fault 5 occurs in the condenser cooling water inlet temperature, and XMV(11) happens to be the condenser cooling water flow. Similarly, of 582 (72.75%) true alarms when detecting Fault 19, (37) attributes 323 alarms to sensor 27, that is, XMV(5). The diagnostic results hint at the direction matrices of Faults 5 and 19, which are $\mathbf{e}_{33}$ and $\mathbf{e}_{27}$, respectively. This further facilitates the use of the diPCA method that is expressed in (17) and assumes known fault directions. Therefore, the diPCA methods with $\mathbf{\Xi}_i = \mathbf{e}_{33}$ and $\mathbf{\Xi}_i = \mathbf{e}_{27}$, respectively, can also be employed. The results together with the other methods are listed in Table VI. It is seen that only one known fault direction suffices for fault detection with high F-measures.

VI. CONCLUSION

This article established a diPCA framework for process monitoring and diagnosis based on the LRT of the PPCA model. The hypothesis testing has the flexibility to incorporate various types of fault directions, including a single direction and mutually orthogonal directions. Consequently, some existing monitoring indices, such as T^2 and Q, are special cases of diPCA monitoring statistics. Moreover, using the identity matrix as the fault direction matrix, a novel combined monitoring index involving both T^2 and Q was proposed. Unlike

the conventional combined index in [17], this new combined statistic does not involve extra parameters and makes statistical sense. As a byproduct, the concise forms of the control limits of the Q statistic and the new combined statistic are suggested, which are sufficiently accurate and easy to derive.

Furthermore, by incorporating composite hypotheses, cdiPCA monitoring statistics are also proposed, which include the T^2-Q scheme as a special case and also lead to a fast monitoring statistic to detect single-sensor faults. Besides speeding fault detection, the (composite) diPCA also facilitates accurate fault diagnosis.

The PPCA model employed here does not take autocorrelation between processes into account, which may be insufficient when monitoring dynamic processes [30], [32]–[34]. Another topic is the nonlinear extension by integrating diPCA with just-in-time learning [35], [36], or with kernel methods [16], [37]. In fact, directional fault information can also be combined with and exploited by other models in various circumstances, such as the hidden Markov models [38] and Bayesian networks [39] for fault classification. These topics deserve future research.

APPENDIX A
PROOF OF THEOREM 1

Consider the LRT for testing the null hypothesis H_0 against the alternative H_1. Let $\boldsymbol{\Theta}_0$ and $\boldsymbol{\Theta}_1$ be the subsets of the parameter spaces associated with H_0 and H_1, respectively, and let $\boldsymbol{\Gamma} = \boldsymbol{\Theta}_0 \cup \boldsymbol{\Theta}_1$. Denote the dimensions of $\boldsymbol{\Theta}_0$ and $\boldsymbol{\Gamma}$ by v_0 and v, respectively. Casella and Berger [28, Th. 10.3.3] stated that the LRT statistic for testing H_0 against H_1 asymptotically follows the chi-square distribution with d.f.$= v - v_0$, that is, $\chi^2_{v-v_0}$.

The expression in (17) is the LRT statistic for testing hypothesis (13), which is rewritten as follows:

$$H_0 : \boldsymbol{\mu} = \mathbf{0} \quad \text{versus} \quad H_1 : \boldsymbol{\mu} = \boldsymbol{\Xi}_i \mathbf{f}_i. \tag{45}$$

Here, the dimension of $H_0 : \boldsymbol{\mu} = \mathbf{0}$ is 0, which is just a single point; whereas, the dimension of $H_1 : \boldsymbol{\mu} = \boldsymbol{\Xi}_i \mathbf{f}_i$ is r_i, where r_i is the rank of the fault direction matrix $\boldsymbol{\Xi}_i$ and the rank of the column space of $\boldsymbol{\Xi}_i$. According to [28, Th. 10.3.3], the LRT statistic in (17) asymptotically follows $\chi^2_{r_i}$.

Specifically, if $\boldsymbol{\Xi}_i = \widetilde{\boldsymbol{U}}$ with rank $p - q$, the LRT statistic in (17) leads to $(1/\sigma)Q$ and, therefore, $(1/\sigma)Q$ asymptotically follows χ^2_{p-q}. Also, if $\boldsymbol{\Xi}_i = \mathbf{I}_p$ with rank p, the LRT statistic in (17) leads to W in (21) and, therefore, W asymptotically follows χ^2_p. This concludes the proof of Theorem 1.

APPENDIX B
PROOF OF THEOREM 2

First, we prove for any $p \times r$ matrix $\boldsymbol{G}$ with rank$(\boldsymbol{G}) = r$ and any $p \times l$ matrix $\boldsymbol{H}$ with rank$(\boldsymbol{H}) = l$, there is

$$\boldsymbol{H}^T\boldsymbol{H} \geq \boldsymbol{H}^T\boldsymbol{G}\big(\boldsymbol{G}^T\boldsymbol{G}\big)^{-1}\boldsymbol{G}^T\boldsymbol{H}. \tag{46}$$

To this end, construct the following matrix:

$$\mathbf{B} = \mathbf{I}_p - \boldsymbol{G}\big(\boldsymbol{G}^T\boldsymbol{G}\big)^{-1}\boldsymbol{G}^T. \tag{47}$$

It can be verified that $\mathbf{B}$ is a symmetric and idempotent matrix, satisfying $\mathbf{B} = \mathbf{B}^T = \mathbf{B}^2$. Therefore, $\mathbf{B}$ is positive semidefinite, leading to

$$\mathbf{I}_p - \boldsymbol{G}\big(\boldsymbol{G}^T\boldsymbol{G}\big)^{-1}\boldsymbol{G}^T \geq \mathbf{0}. \tag{48}$$

By multiplying $\boldsymbol{H}^T$ and $\boldsymbol{H}$ on both sides of (48), there is

$$\boldsymbol{H}^T\Big(\mathbf{I}_p - \boldsymbol{G}\big(\boldsymbol{G}^T\boldsymbol{G}\big)^{-1}\boldsymbol{G}^T\Big)\boldsymbol{H} \geq \mathbf{0} \tag{49}$$

which is equivalent to (46).

Furthermore, take

$$\boldsymbol{G} = \boldsymbol{\Sigma}^{-\frac{1}{2}}\boldsymbol{\Xi}_j, \quad \boldsymbol{H} = \boldsymbol{\Sigma}^{-\frac{1}{2}}\boldsymbol{\Xi}_i. \tag{50}$$

By substituting $\boldsymbol{G}$ and $\boldsymbol{H}$ in (50) into (46), there is

$$\boldsymbol{\Xi}_i{}^T\boldsymbol{\Sigma}^{-1}\boldsymbol{\Xi}_i \geq \boldsymbol{\Xi}_i{}^T\boldsymbol{\Sigma}^{-1}\boldsymbol{\Xi}_j\Big(\boldsymbol{\Xi}_j{}^T\boldsymbol{\Sigma}^{-1}\boldsymbol{\Xi}_j\Big)^{-1}\boldsymbol{\Xi}_j{}^T\boldsymbol{\Sigma}^{-1}\boldsymbol{\Xi}_i. \tag{51}$$

Notice $\mathbf{x} = \boldsymbol{\Xi}_i\mathbf{f}_i$ with arbitrary $\mathbf{f}_i$, and finally, we have

$$\begin{aligned}&\mathbf{f}_i^T\boldsymbol{\Xi}_i{}^T\boldsymbol{\Sigma}^{-1}\boldsymbol{\Xi}_i\mathbf{f}_i \\ &\quad\geq \mathbf{f}_i^T\boldsymbol{\Xi}_i{}^T\boldsymbol{\Sigma}^{-1}\boldsymbol{\Xi}_j\Big(\boldsymbol{\Xi}_j{}^T\boldsymbol{\Sigma}^{-1}\boldsymbol{\Xi}_j\Big)^{-1}\boldsymbol{\Xi}_j{}^T\boldsymbol{\Sigma}^{-1}\boldsymbol{\Xi}_i\mathbf{f}_i.\end{aligned} \tag{52}$$

This concludes the proof of Theorem 2.

ACKNOWLEDGMENT

The authors would like to thank the Editor-in-Chief, the Associate Editor, and five anonymous referees for their many helpful comments that have resulted in significant improvements in this article.

REFERENCES

[1] M. Kordestani, M. Saif, M. E. Orchard, R. Razavi-Far, and K. Khorasani, "Failure prognosis and applications—A survey of recent literature," *IEEE Trans. Rel.*, early access, Sep. 17, 2016, doi: 10.1109/TR.2019.2930195.

[2] M. Kordestani, K. Salahshoor, A. A. Safavi, and M. Saif, "An adaptive passive fault tolerant control system for a steam turbine using a PCA based inverse neural network control strategy," in *Proc. IEEE World Autom. Congr. (WAC)*, 2018, pp. 40–45.

[3] T. Yi, Y. Xie, H. Zhang, and X. Kong, "Insulation fault diagnosis of disconnecting switches based on wavelet packet transform and PCA-IPSO-SVM of electric fields," *IEEE Access*, vol. 8, pp. 176676–176690, 2020.

[4] M. Rezamand, M. Kordestani, R. Carriveau, D. S.-K. Ting, and M. Saif, "A new hybrid fault detection method for wind turbine blades using recursive PCA and wavelet-based PDF," *IEEE Sensors J.*, vol. 20, no. 4, pp. 2023–2033, Feb. 2020.

[5] M. Schmid, H.-G. Kneidinger, and C. Endisch, "Data-driven fault diagnosis in battery systems through cross-cell monitoring," *IEEE Sensors J.*, vol. 21, no. 2, pp. 1829–1837, Jan. 2021.

[6] P. Zhou, R. Zhang, J. Xie, J. Liu, H. Wang, and T. Chai, "Data-driven monitoring and diagnosing of abnormal furnace conditions in blast furnace ironmaking: An integrated PCA-ICA method," *IEEE Trans. Ind. Electron.*, vol. 68, no. 1, pp. 622–631, Jan. 2021.

[7] I. T. Jolliffe, *Principal Component Analysis*, 2nd ed. New York, NY, USA: Springer-Verlag, 2002.

[8] H. Wang, M. Chen, X. Shi, and N. Li, "Principal component analysis for normal-distribution-valued symbolic data," *IEEE Trans. Cybern.*, vol. 46, no. 2, pp. 356–365, Feb. 2016.

[9] S. J. Qin, "Statistical process monitoring: Basics and beyond," *J. Chemometrics*, vol. 17, nos. 8–9, pp. 480–502, 2003.

[10] S. J. Qin, "Survey on data-driven industrial process monitoring and diagnosis," *Annu. Rev. Control*, vol. 36, no. 2, pp. 220–234, Dec. 2012.

[11] Z. Ge, Z. Song, and F. Gao, "Review of recent research on data-based process monitoring," *Ind. Eng. Chem. Res.*, vol. 52, no. 10, pp. 3543–3562, 2013.

[12] S. Yin, S. X. Ding, X. Xie, and H. Luo, "A review on basic data-driven approaches for industrial process monitoring," *IEEE Trans. Ind. Electron.*, vol. 61, no. 11, pp. 6418–6427, Nov. 2014.
[13] B. D. Ketelaere, M. Hubert, and E. Schmitt, "Overview of PCA-based statistical process-monitoring methods for time-dependent, high-dimensional data," *J. Qual. Technol.*, vol. 47, no. 4, pp. 318–335, 2015.
[14] C. F. Alcala and S. J. Qin, "Reconstruction-based contribution for process monitoring," *Automatica*, vol. 45, no. 7, pp. 1593–1600, 2009.
[15] J. A. Westerhuis, S. P. Gurden, and A. K. Smilde, "Generalized contribution plots in multivariate statistical process monitoring," *Chemometr. Intell. Lab. Syst.*, vol. 51, no. 1, pp. 95–114, 2000.
[16] C. F. Alcala and S. J. Qin, "Reconstruction-based contribution for process monitoring with kernel principal component analysis," *Ind. Eng. Chem. Res.*, vol. 49, no. 17, pp. 7849–7857, 2010.
[17] H. Yue and S. J. Qin, "Reconstruction based fault identification using a combined index," *Ind. Eng. Chem. Res.*, vol. 40, no. 20, pp. 4403–4414, 2001.
[18] A. Raich and A. Cinar, "Statistical process monitoring and disturbance diagnosis in multivariate continuous processes," *AIChE J.*, vol. 42, no. 4, pp. 995–1009, 1996.
[19] J. E. Jackson and G. Mudholkar, "Control procedures for residuals associated with principal component analysis," *Technometrics*, vol. 21, no. 3, pp. 341–349, Aug. 1979.
[20] F. Harrou, M. N. Nounou, H. N. Nounou, and M. Madakyaru, "Statistical fault detection using PCA-based GLR hypothesis testing," *J. Loss Prevent. Process Ind.*, vol. 26, no. 1, pp. 129–139, 2013.
[21] M. Z. Sheriff, M. Mansouri, M. N. Karim, H. Nounou, and M. Nounou, "Fault detection using multiscale PCA-based moving window GLRT," *J. Process Control*, vol. 54, pp. 47–64, Jun. 2017.
[22] M. E. Tipping and C. M. Bishop, "Probabilistic principal component analysis," *J. Roy. Stat. Soc. B*, vol. 61, no. 3, pp. 611–622, 1999.
[23] J. Zhang, H. Chen, S. Chen, and X. Hong, "An improved mixture of probabilistic PCA for nonlinear data-driven process monitoring," *IEEE Trans. Cybern.*, vol. 49, no. 1, pp. 198–210, Jan. 2019.
[24] D. Kim and I. B. Lee, "Process monitoring based on probabilistic PCA," *Chemometr. Intell. Lab. Syst.*, vol. 67, no. 2, pp. 109–123, 2003.
[25] Z. Ge, "Process data analytics via probabilistic latent variable models: A tutorial review," *Ind. Eng. Chem. Res.*, vol. 57, pp. 12646–12661, Aug. 2018.
[26] J. Zhao, "Efficient model selection for mixtures of probabilistic PCA via hierarchical BIC," *IEEE Trans. Cybern.*, vol. 44, no. 10, pp. 1871–1883, Oct. 2014.
[27] R. Raveendran, H. Kodamana, and B. Huang, "Process monitoring using a generalized probabilistic linear latent variable model," *Automatica*, vol. 96, pp. 73–83, Oct. 2018.
[28] G. Casella and R. L. Berger, *Statistical Inference*, 2nd ed. Singapore: Cengage Learn., 2001.
[29] P. Embrechts, C. Kluppelberg, and T. Mikosch, *Modelling Extremal Events for Insurance and Finance*. Berlin, Germany: Springer-Verlag, 1997.
[30] Y. Dong and S. J. Qin, "A novel dynamic PCA algorithm for dynamic data modeling and process monitoring," *J. Process Control*, vol. 67, pp. 1–11, Jul. 2018.
[31] S. Yin, S. X. Ding, A. Haghani, H. Hao, and P. Zhang, "A comparison study of basic data-driven fault diagnosis and process monitoring methods on the benchmark Tennessee Eastman process," *J. Process Control*, vol. 22, no. 9, pp. 1567–1581, 2012.
[32] G. Li, S. J. Qin, and D. Zhou, "A new method of dynamic latent-variable modeling for process monitoring," *IEEE Trans. Ind. Electron.*, vol. 61, no. 11, pp. 6438–6445, Nov. 2014.
[33] Z. Ge and X. Chen, "Dynamic probabilistic latent variable model for process data modeling and regression application," *IEEE Trans. Control Syst. Technol.*, vol. 27, no. 1, pp. 323–331, Jan. 2019.
[34] L. Zhou, G. Li, Z. Song, and S. J. Qin, "Autoregressive factor analysis models for dynamic process monitoring," *IEEE Trans. Control Syst. Technol.*, vol. 25, no. 1, pp. 366–373, Jan. 2017.
[35] S. Yin, H. Gao, J. Qiu, and O. Kaynak, "Fault detection for nonlinear process with deterministic disturbances: A just-in-time learning based data driven method," *IEEE Trans. Cybern.*, vol. 47, no. 11, pp. 3649–3657, Nov. 2017.
[36] C. Cheng and M. S. Chiu, "Nonlinear process monitoring using JITL-PCA," *Chemometr. Intell. Lab. Syst.*, vol. 76, no. 1, pp. 1–13, 2005.
[37] M. Mansouri, M. Nounou, H. Nounou, and N. Karim, "Kernel PCA-based GLRT for nonlinear fault detection of chemical processes," *J. Loss Prevent. Process Ind.*, vol. 40, pp. 334–347, Mar. 2016.
[38] J. Zhu, Z. Ge, and Z. Song, "HMM-driven robust probabilistic principal component analyzer for dynamic process fault classification," *IEEE Trans. Ind. Electron.*, vol. 62, no. 6, pp. 3814–3821, Jun. 2015.
[39] J. Zheng, J. Zhu, G. Chen, Z. Song, and Z. Ge, "Dynamic Bayesian network for robust latent variable modeling and fault classification," *Eng. Appl. Artif. Intell.*, vol. 89, Mar. 2020, Art. no. 103475.

Jian Li (Member, IEEE) received the B.S. degree in automation from Tsinghua University, Beijing, China, in 2006, and the Ph.D. degree in industrial engineering and logistics management from the Hong Kong University of Science and Technology, Hong Kong, in 2012.

He is currently a Professor with the School of Management, Xi'an Jiaotong University, Xi'an, China. His research interests include statistical process control, data-driven fault detection and diagnosis, industrial big data analytics, and statistical machine learning.

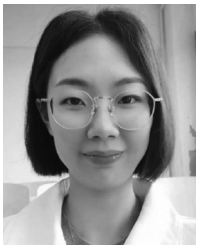

Dong Ding received the B.S. degree in statistics from Nankai University, Tianjin, China, in 2011, and the Ph.D. degree in industrial engineering and decision analytics from the Hong Kong University of Science and Technology, Hong Kong, in 2015.

She is currently an Associate Professor with the School of Management, Xi'an Polytechnic University, Xi'an, China. Her current research interests include quality management, quality engineering, and statistical process control.

Fugee Tsung received the B.Sc. degree from National Taiwan University, Taipei, Taiwan, in 1990, and the M.Sc. and Ph.D. degrees from the University of Michigan, Ann Arbor, MI, USA, in 1993 and 1997, respectively.

He is currently a Chair Professor with the Department of Industrial Engineering and Decision Analytics and the Director of the Quality and Data Analytics Laboratory, Hong Kong University of Science and Technology, Hong Kong. His research interests include quality analytics in advanced manufacturing and service processes, industrial big data, and statistical process control, monitoring, and diagnosis.

Dr. Tsung has been an elected Academician of the International Academy for Quality, a Fellow of the Institute of Industrial Engineers, a Fellow of the American Statistical Association, a Fellow of the American Society for Quality, and an elected member of the International Statistical Institute, based on his pioneer contribution to Quality Analytics research and education.